

This copy of the ESI replaces the previous version published on 29 March 2021

## Supplementary Information for

### Influence of Mg-doping in ZnO Photoanodes on their Characteristics in Dye-Sensitized Solar Cells

*Andreas Ringleb<sup>a</sup>, Raffael Ruess<sup>b</sup>, Nico Hofeditz<sup>c</sup>, Wolfram Heimbrodt<sup>c</sup>, Tsukasa Yoshida<sup>d</sup> and Derck Schlettwein<sup>a,\*</sup>*

<sup>a</sup> Institute of Applied Physics and Center for Materials Research, Justus-Liebig-University  
Heinrich-Buff-Ring 16, D-35392 Giessen, Germany

<sup>b</sup> Institute of Physical Chemistry, Justus-Liebig-University Giessen,  
Heinrich-Buff-Ring 16, 35392 Giessen, Germany

<sup>c</sup> Department of Physics and Materials Science Centre, Philipps-University of Marburg  
Renthof 5, 35032 Marburg, Germany

<sup>d</sup> Department of Chemistry and Chemical Engineering, Faculty of Engineering, Yamagata  
University, Jonan 4-3-16, Yonezawa, Yamagata 992-8510, Japan

Table S1 - Mg-concentration in the precursor solution  $[Mg_{sol}]$  compared to that measured in the thin films  $[Mg_{TF}]$  by energy-dispersive X-ray spectroscopy (EDX) and the corresponding lattice parameters determined from XRD.

$[Mg_{sol}] / \%$	$[Mg_{TF}] / \%$	$c / \text{Å}$	$a / \text{Å}$
0	0	5.2115	3.2476
5	5.2	5.2074	3.2538
10	11.5	5.2034	3.2554
20	18.1	5.1979	3.2559

Table S2 - Extrapolated band gaps from Tauc-plots for nanoparticulate and thin film MZO depending on the Mg-concentration.

Mg-content / %	Band gap / eV	
	NP	TF
0	3.28	3.27
5	3.35	3.34
10	3.42	3.39
20	3.52	3.50

Table S3 - Absorbance maximum and the calculated values for the quantum efficiency (QE) in the maximum.

Mg	NP		TF		CS	
	$abs_{max}$	$QE_{max} / \%$	$abs_{max}$	$QE_{max} / \%$	$abs_{max}$	$QE_{max} / \%$
0	0.84	71.4	0.16	97.5	1.1	63.5
5	0.83	74.2	0.15	114	1.08	62.5
10	0.83	35.8	0.18	67.9	1.05	56.7
20	0.86	8.8	0.17	24.6	1.11	39.7

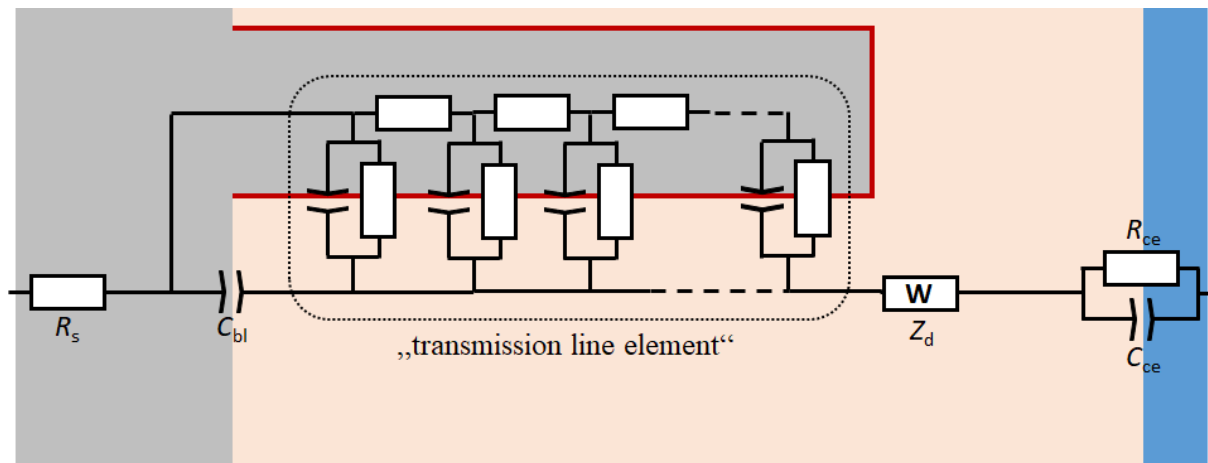


Figure S1 - Equivalent electrical circuit used for the fitting of the EIS data.

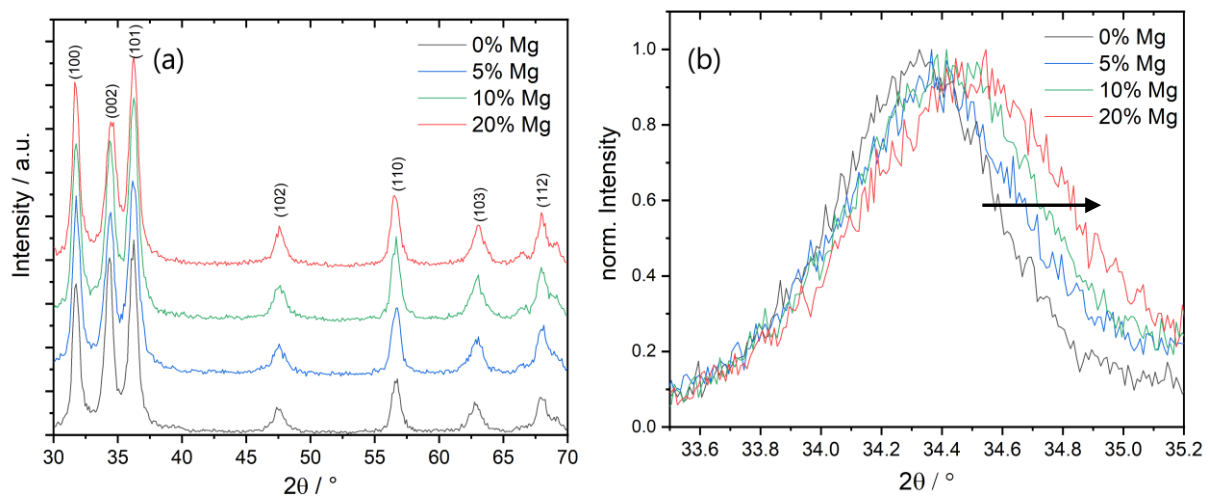


Figure S2 - XRD of MZO TF samples of varying Mg-concentration. (a) overview of MZO TF with 0, 5, 10 and 20% Mg. The typical ZnO wurtzite reflexes are indexed. (b) detail of the (002) reflex and the shift upon Mg-doping towards larger angles is indicated by the arrow.

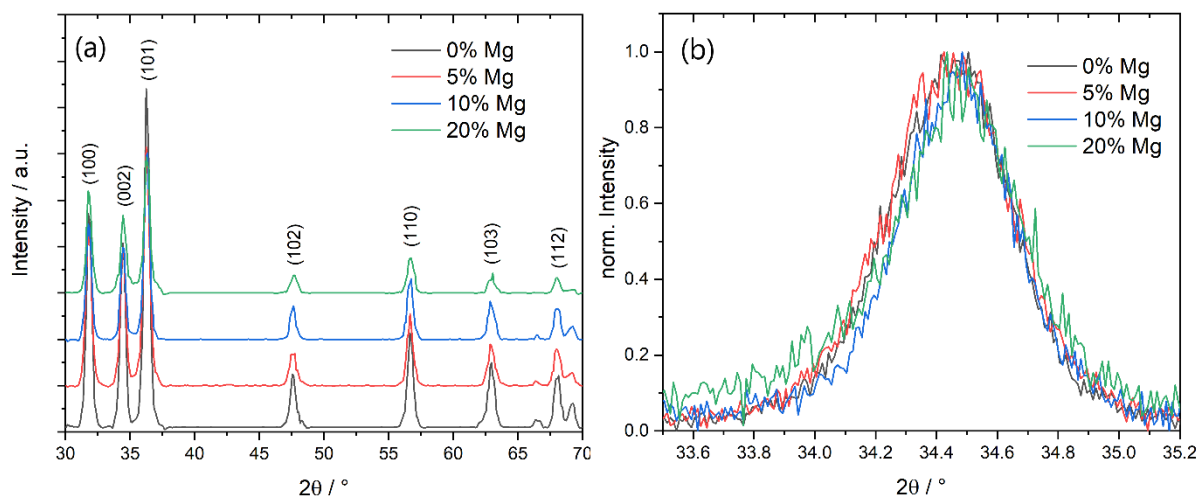


Figure S3 - XRD of MZO CS samples of varying Mg-concentration. (a) overview of MZO CS with 0, 5, 10 and 20% Mg. The typical ZnO wurtzite reflexes are indexed. (b) detail of the (002) reflex which was found at constant angle because it is dominated by the large amount of the undoped ZnO core compared to small contributions by the thin MZO shell.

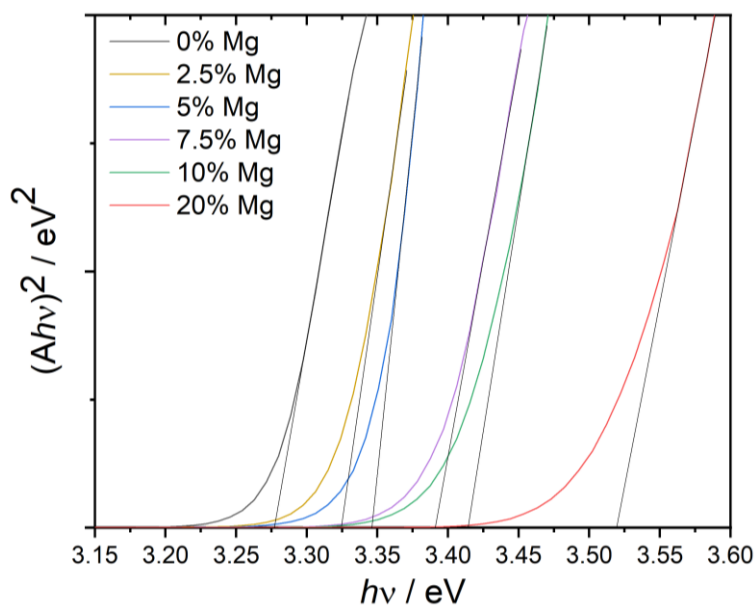


Figure S4 - Tauc-plot of the optical absorption spectra of MZO nanoparticles with varying Mg-concentration with fits to the linear part.

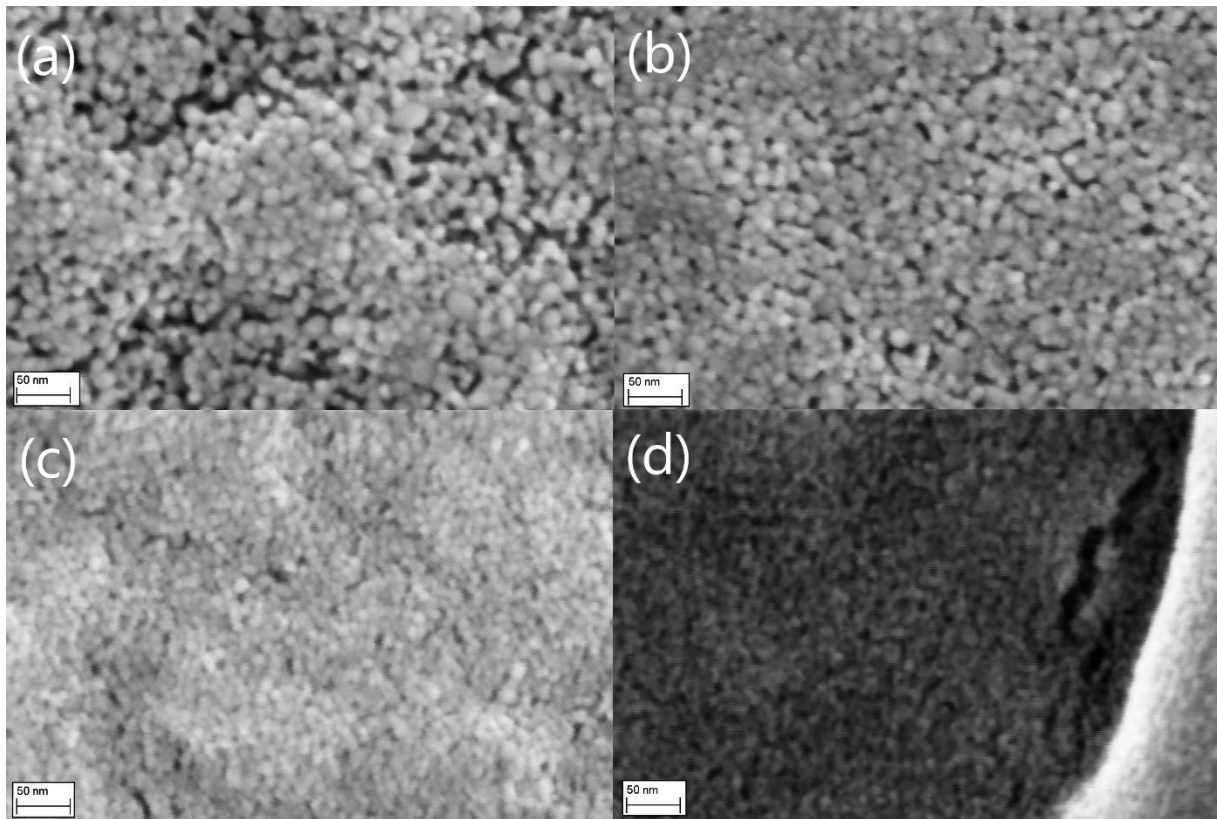


Figure S5 - SEM images of MZO thin films (TF) including (a) 0% Mg, (b) 5% Mg, (c) 10% Mg and (d) 20% Mg at 200k times magnification.

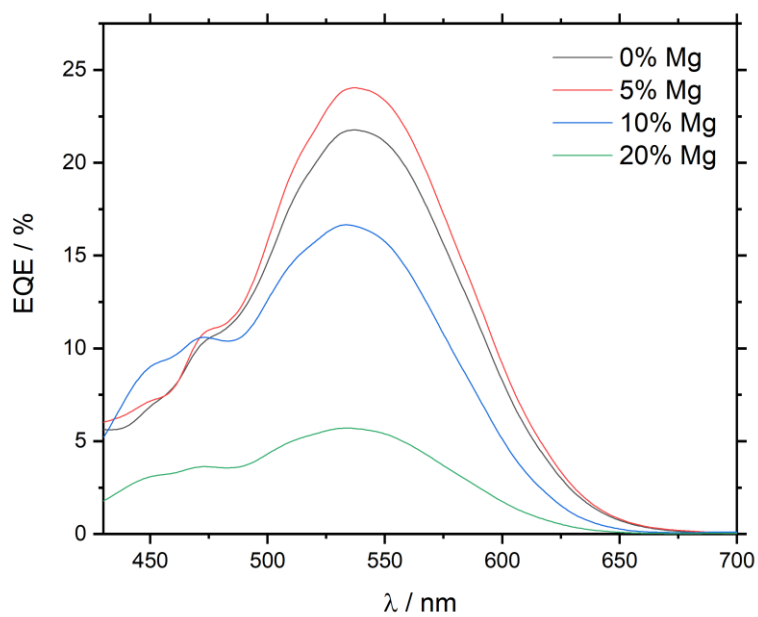


Figure S6 - EQE spectra of TF-type photoanodes of varying Mg-concentrations.

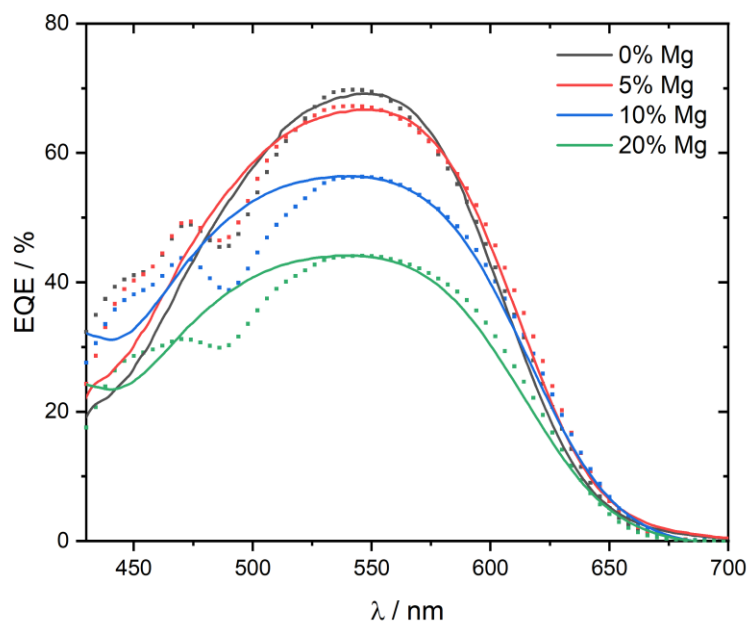


Figure S7 - EQE spectra (dots) and fits (lines) of CS-type photoanodes of varying Mg-concentration.

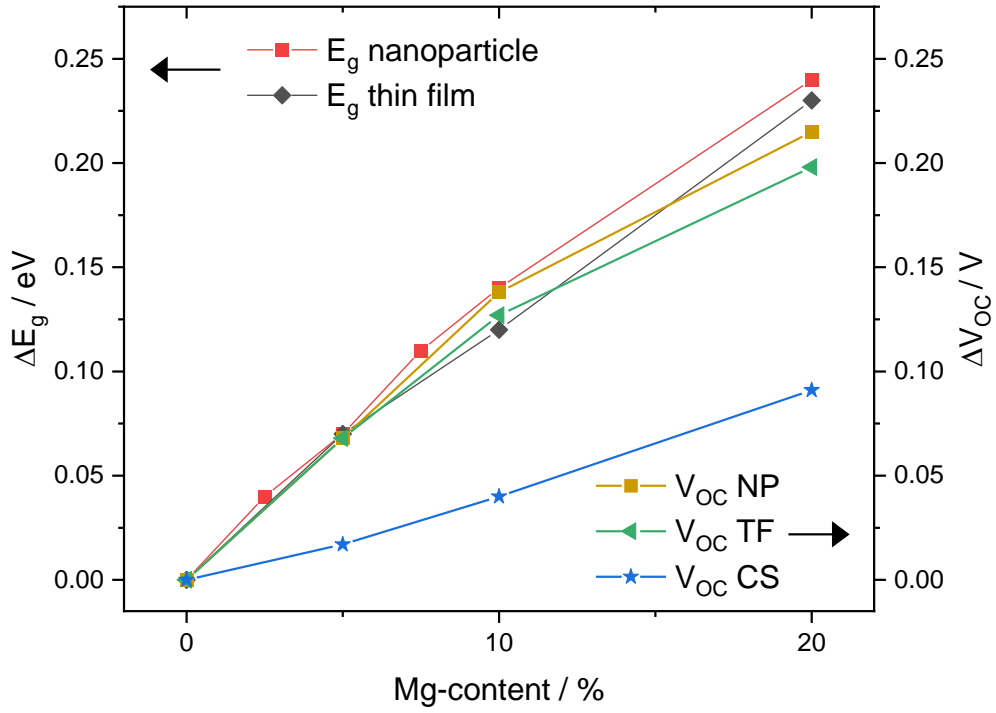


Figure S8 - Comparison between the increase in the band gap  $\Delta E_g$  determined from optical spectroscopy and the increase in open-circuit voltage  $\Delta V_{OC}$  caused by Mg-doping compared to pure ZnO.

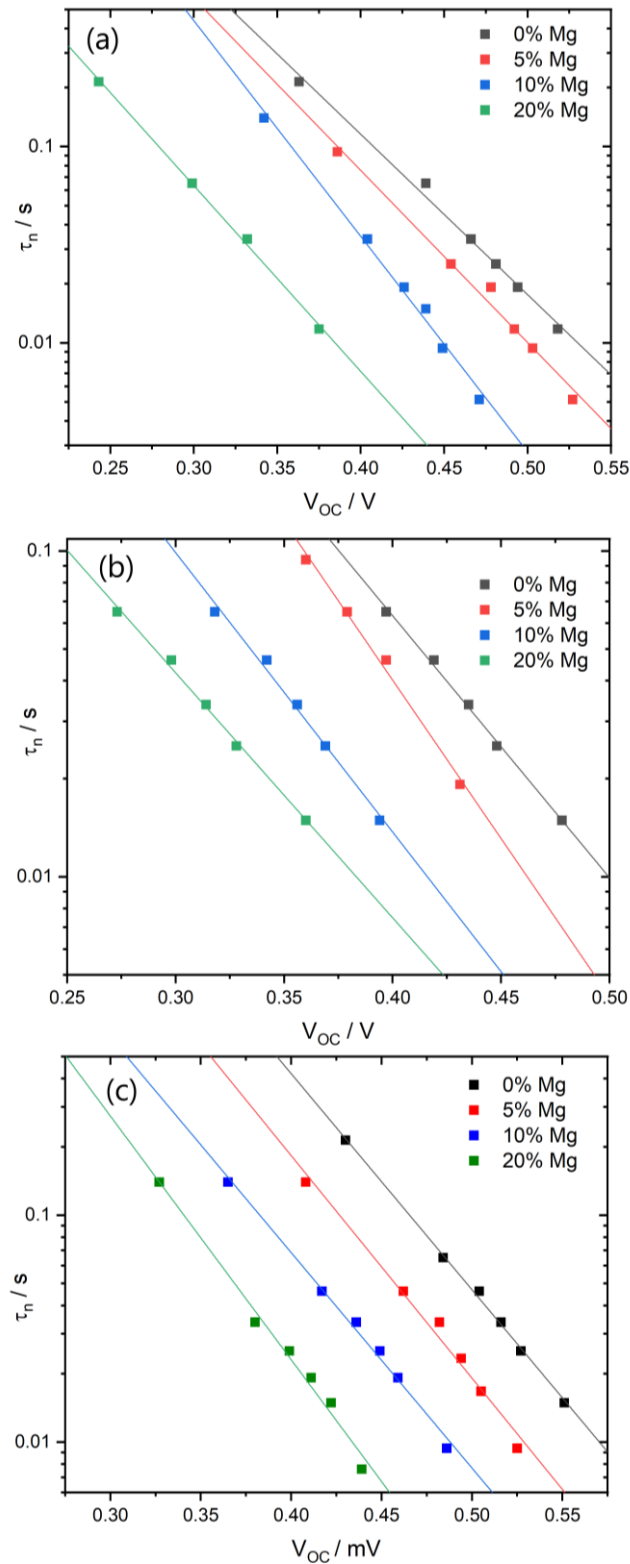


Figure S9 - Electron lifetimes  $\tau_n$  derived from IMVS measurements at various light intensities for (a) NP-, (b) TF- and (c) CS-type photoanodes. The experimental data for the 5%, 10% and 20% MZO photoanodes has been normalized relative to pure ZnO by the increase of the band gap  $\Delta E_g$ , as discussed in the text.



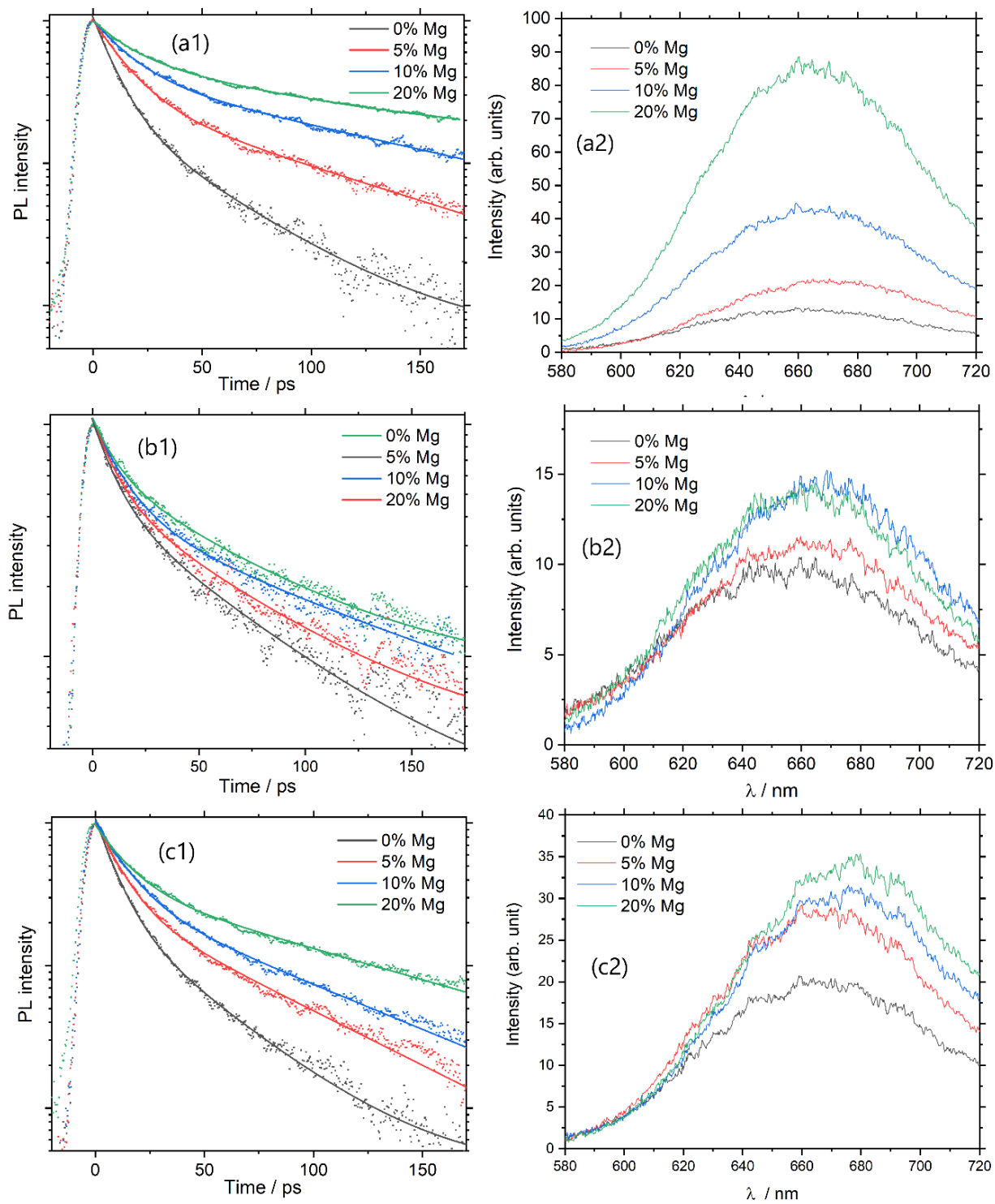


Figure S10 - Bi-exponential fits of the measured TRPL spectra for (a1) NP-, (b1) TF- and (c1) CS-type photoanodes, as well as the integrated PL spectra for (a2) NP-, (b2) TF- and (c2) CS-type photoanodes.